CU Dent J. 2017;40:27-38

Original Article

Evaluation of technical image quality and radiation dose of a Thai cone-beam CT scanner

Ruben Pauwels, Ph.D.[1,2]
Saowapak Thongvigitmanee, Ph.D.[3]
Sorapong Aootaphao, M.S.[3]
Chalinee Thanasupsombat, M.S.[3]
Walita Narkbuakaew, D.Eng.[3]
Reinhilde Jacobs, Ph.D.[2]
Hilde Bosmans, Ph.D.[4]
Soontra Panmekiate, Ph.D.[1]
Pairash Thajchayapong, Ph.D.[5]

[1]Department of Radiology, Faculty of Dentistry, Chulalongkorn University, Bangkok, Thailand
[2]OMFS-IMPATH Research Group, Department of Imaging and Pathology, Biomedical Sciences Group, Catholic University of Leuven, Leuven, Belgium
[3]X-Ray CT and Medical Imaging Laboratory, Biomedical Electronics and Systems Research Unit, National Electronics and Computer Technology Center, National Science and Technology Development Agency, Pathumthani, Thailand
[4]Medical Physics & Quality Assessment, Department of Imaging and Pathology, Biomedical Sciences Group, Catholic University of Leuven, Leuven, Belgium
[5]National Science and Technology Development Agency, Pathumthani, Thailand

Abstract

Objectives The aim of this study is to evaluate the technical image quality and radiation dose of the DentiiScan 2.0 cone-beam computed tomography (CBCT) scanner before widespread clinical use.

Materials and methods Image quality was measured for 4 scanning protocols of the DentiiScan 2.0, using 2 dedicated test objects: the SEDENTEXCT IQ phantom and the QRM-ConeBeam phantom. The following image quality parameters were evaluated: contrast-detail, contrast-to-noise ratio (CNR), spatial resolution, grey value uniformity, metal artefacts, and geometric accuracy. Radiation dose was measured using a calibrated ionization chamber placed at the isocenter of rotation, allowing for the calculation of the dose-area product (DAP).

Results For contrast-detail, scores were almost identical for all protocols, with all 5 rods being distinguishable for aluminium, air, hydroxyapatite 200 mg/cm^3, polytetrafluorethylene, and low-density polyethylene. CNR values were commensurate with the contrast-detail results. Visual evaluation of the line pair patterns revealed considerable differences between scanning protocols. Some consistency between voxel size and sharpness could be seen. High grey value uniformity was found for Protocols 1-3; for Protocol 4 the uniformity was slightly worse. There was no difference in artefact severity between scanning protocols. For geometric accuracy, average errors between 0.04 and 0.08 mm were found, indicating high accuracy. The dose-area product was 897.1 mGy.cm^2 for Protocol 1, 1058.4 mGy.cm^2 for Protocol 2, 474.1 mGy.cm^2 for Protocol 3, and 424.4 mGy.cm^2 for Protocol 4.

Conclusion The DentiiScan 2.0 showed adequate performance in terms of technical image quality, and a low radiation dose compared with other CBCT models. The protocol with the smallest FOV provided the best balance between image quality and dose.

(CU Dent J. 2017;40:27-38)

Key words: *cone-beam computed tomography, dentistry, image quality, radiation dose, Thailand*

Correspondence: Ruben Pauwels, ruben.pauwels@kuleuven.be & pauwelsruben@hotmail.com

Introduction

Cone-beam computed tomography (CBCT) was introduced in dentistry in 1996. CBCT allows for three-dimensional imaging of the dentomaxillofacial region, and has thus become a widely used imaging modality for implant planning, endodontic diagnosis, and various other clinical applications (Kamburoğlu 2015).

Currently, over 50 different CBCT scanner models are in clinical use (Nemtoi et al., 2013). These models exhibit considerable differences in terms of image quality (Pauwels et al., 2012a) and radiation dose (Pauwels et al., 2012b). These differences are partly due to the use of a wide range in scanning parameters (e.g. kV, mAs, field of view, voxel size). Therefore, it is essential to evaluate the performance of a CBCT unit before and during clinical use, ensuring that it meets minimal requirements in terms of image quality and that radiation dose is optimized (Kiljunen et al., 2015).

Although the use of CBCT is growing exponentially, the price of the equipment remains an issue, particularly in developing countries. Recently, a CBCT machine, called DentiiScan was developed by the National Electronics and Computer Technology Center (NECTEC) and the National Metal and Materials Technology Center (MTEC) under the National Science and Technology Development Agency (NSTDA) of Thailand (Thongvigitmanee et al., 2013). The primary aim of this development is to bring an affordable yet high-performance CBCT model to the local market. Furthermore, a locally produced CBCT would allow for an optimal after-sales service, including user training and maintenance. The first version of the DentiiScan (DentiiScan 1.1) has undergone clinical testing at different centres, and based on the outcome of this evaluation, DentiiScan 2.0 was developed. Before clinical validation of this new model, the technical image quality (in terms of sharpness, contrast, noise, artefacts and geometric accuracy) as well as the radiation dose should be assessed.

The aim of this study is to evaluate the technical image quality and radiation dose of the DentiiScan 2.0 CBCT before widespread clinical use.

Materials and methods

The DentiiScan 2.0 (Fig. 1) is a compact CBCT unit (1m × 1.3m × 2.3m) in which the patient is scanned in a standing, sitting or wheelchair position. Four imaging protocols are predetermined by the manufacturer, with varying field of view (FOV) size, mAs, and voxel size. Technical specifications of the DentiiScan 2.0, as well as exposure parameters for each of the four imaging protocols, are listed in Table 1. Aside from differences in FOV size, it can be noticed that Protocol 1 uses a lower mAs, which is commensurate to its larger voxel size.

1. *Image quality*

The SEDENTEXCT IQ phantom (Leeds Test Objects, Boroughbridge, UK) was used for the evaluation of technical image quality (Fig. 2). In addition, the QRM-ConeBeam phantom (QRM Quality Assurance in Radiology and Medicine GmbH, Moehrendorf, Germany) was used for measurement of geometric accuracy (Fig. 3).

Figure 1 The DentiiScan 2.0 CBCT scanner

Figure 2 SEDENTEXCT IQ phantom used for technical image quality analysis

Figure 3 QRM–ConeBeam phantom used for geometric accuracy analysis

Table 1 Technical specifications and scanning protocols of the DentiiScan 2.0

General specifications				
Detector type	Amorphous Silicon Flat Panel			
Detector size	20 × 25 cm			
Tube voltage	90 kVp			
Focal spot	0.5 mm			
Scanning protocols				
	Protocol 1	Protocol 2	Protocol 3	Protocol 4
mA	6	9	9	9
Exposure time (s)	5.76	6.84	6.84	6.84
mAs	34.56	61.56	61.56	61.56
Scan time (s)	18	18	18	18
Voxel size (mm)	0.4	0.25	0.2	0.2
FOV diameter (mm)	160	150	120	80
FOV height (mm)	130	105	60	80

The SEDENTEXCT IQ phantom was developed specifically for use in quality assurance of dental CBCT, and has been previously described in detail (Pauwels et al., 2011). It consists of a polymethyl-methacrylate (PMMA) cylinder of 160 mm diameter and 177 mm height, containing a variety of cylindrical inserts that allow for the evaluation of the different image quality metrics, as described below. The phantom was scanned using four protocols (Table 1). For Protocols 1-2, the phantom was scanned in a central position. For Protocols 3-4, the phantom was positioned non-centrally in order to mimic a dental scan; this implies that separate scans were obtained of each section of the phantom. Image quality analysis was performed using ImageJ (US National Institutes of Health, Bethesda, MD, USA).

1.1 *Contrast-detail*

This insert consists of 5 cylindrical rods, with a diameter between 1 and 5 mm, embedded in PMMA (Pauwels et al., 2012a). Eight contrast-detail inserts, containing different materials [aluminium, air, hydroxyapatite (HA) 50 mg/cm^3, HA 100 mg/cm^3, HA 200 mg/cm^3, polytetrafluoroethylene (PTFE), polyoxymethylene (POM), and low-density polyethylene (LDPE)] were used. The number of rods that can be distinguished on an axial slice through each insert represent the contrast-detail performance of the scan. The number of visible rods for each insert was counted by an experienced observer.

1.2 *Contrast-to-noise ratio (CNR)*

The CNR compares the difference in grey values between two materials with different attenuation (i.e. contrast) with the random fluctuation of grey values within voxels corresponding to a homogeneous material (i.e. noise). Two types of inserts were used for CNR measurements. The first type contained a 10 mm cylinder embedded in PMMA. For this insert, five materials were used: aluminium, air, HA 50, HA 100 and HA 200. A second type of insert contained slabs of different materials (incl. PTFE, POM, and LDPE) stacked on top of each other. The mean grey value (MGV) and standard deviation of grey values (SD) within a region of interest (ROI) was measured for each material *m*, and CNR_m was calculated as:

$$CNR_m = \frac{|MGV_m - MGV_{ref}|}{\sqrt{(SD_m^2 + SD_{ref}^2)}}$$

with MGV_{ref} and SD_{ref} being measured on a reference material (Pauwels et al., 2014). For aluminium, air and HA, PMMA was used as a reference material. For PTFE and POM, LDPE was used as a reference material, as there was no PMMA in this insert.

All CNR measurements were performed by the same observer. To ensure accuracy and reproducibility of ROI placement, a semi-automatic script was used which required the observer to select a single reference point in the image, after which ROIs of identical size were placed relative to this reference point.

1.3 *Line pairs (spatial resolution)*

This insert consisted of a line pair pattern using alternating slabs of aluminium and polymer with decreasing thickness and intervals (i.e. 10 groups of 3 line pairs each, from 1 lp/mm to 10 lp/mm) (Pauwels et al., 2012a, Widmann et al., 2017). Separate inserts were used in order to evaluate the spatial resolution in the axial and trans-axial planes. Visual analysis of the line pair patterns was performed separately in the axial and coronal planes by an experienced observer. The ability to distinguish individual lines in the first two groups of line pairs was evaluated (0: not distinguishable, 0.5: partially distinguishable, 1: distinguishable). The number of visible line pair groups (each consisting of three line pairs) was counted (0: no visible groups, 1: one group visible, ..., 10: all groups visible). Furthermore, subjective scores were provided on overall sharpness (0: poor, 1: moderate, 2: high) and noise (0: high, 1: moderate, 2: low); for both parameters, scores were defined as such that a change in score should represent an expected and relevant shift in diagnostic image quality. A total score (min. 0, max. 16) was calculated for the axial and trans-axial views.

1.4 *Uniformity*

Uniformity refers to the stability of grey values throughout the FOV. For this analysis, five cylindrical regions of interest (ROI) (anterior, posterior, left, right, center) were determined in the homogeneous PMMA section of the SEDENTEXCT phantom. A script enabling automatic ROI size and placement was made for this evaluation, in order to ensure reproducibility of measurements. Using the script, the diameter of each ROI was equalized to 20% of the FOV diameter, the central ROI was in the exact centre of the FOV, and the four peripheral ROIs were positioned exactly halfway between the centre and edge of the FOV.

The largest difference between two ROIs (expressed as absolute grey values, percentage of the grey value range between air and PMMA, and signal difference to noise ratio) was calculated. In addition, the difference between the central region and the four peripheral regions was calculated using the same parameters.

1.5 *Metal artefacts*

The severity of metal artefacts was evaluated using inserts containing three in-line rods (5.15 mm diameter). Two inserts were used, containing titanium and lead. Analysis was done as detailed in a prior publication (Pauwels et al., 2013). The standard deviation (SD_M) of grey values in the insert containing the rods (excluding the rods themselves) as well as the actual grey value range GVR (i.e. the difference between the lowest and highest grey value found in the scan) was measured. The following formula was then used to obtain the normalized SD (SD_{norm}):

$$SD_{norm} = 100 * \frac{SD_M * \frac{4096}{GVR}}{2048}$$

Using this calculation, the SD is normalized to a value corresponding to a 12-bit image (i.e. with a range of 4096 grey values), and expressed as the percentage of

the maximum possible standard deviation for 12-bit images (i.e. 2048). Therefore, SD_{norm} can range between 0 and 100, allowing for a more straightforward interpretation and intercomparison.

1.6 *Geometric accuracy*

For this measurement, the QRM-ConeBeam phantom was used. It contains a grid of holes with a diameter of 3 mm and a spacing of 10 mm. Linear measurements were performed in the anterior-posterior and left-right directions, both from one edge of the field of view to the other edge. Each direction was measured using two combinations of holes, repeated three times each. Deviations were calculated in absolute values (average and maximum, mm) and as a percentage of the measured distance.

2. *Radiation dose*

Dose-area product (DAP) was estimated by measuring the absorbed dose in air at the isocenter (i.e. the central point of the FOV) using a 10X6-6 ion chamber and Accu-Gold Digitizer (Radcal, Monrovia, CA, USA) and multiplying this value with the cross-sectional area of the X-ray beam at the isocenter. Seeing that this measurement does not take inhomogeneities in intensity of the X-ray beam into account (e.g. due to the use of non-flat tube filtration, or due to the heel effect), its accuracy was verified by comparing it with a direct DAP measurement using a DAPcheck Plus meter (Radcal, Monrovia, CA, USA) in 'scout' mode, showing a deviation of 6% between calculated and actual DAP.

Results

Image quality

Table 2 shows the image quality results from the SEDENTEXCT IQ phantom (i.e. all results except geometric accuracy).

For contrast-detail, scores were almost identical for all protocols, with all five rods being distinguishable for aluminium, air, HA 200, PTFE and LDPE, four rods being visible for POM, and zero rods for HA 50 (Fig. 4). The only difference between protocols was found for HA 100, for which Protocol 1 revealed three rods, and all other protocols showed four rods.

Contrast-to-noise ratio was generally the highest for Protocol 2, despite its small voxel size. CNR values were commensurate with differences in attenuation between the material and background, with aluminium showing the highest overall CNR, and HA 50 the lowest. Comparing the CNR results with the contrast-detail findings, it could be seen that a CNR of 1.5 or below implied that the 1-mm rod could no longer be distinguished, a CNR of 0.9 or below implied that the 2-mm rod could no longer be distinguished, and a CNR of 0.4 or below implied that none of the rods could be distinguished.

Visual evaluation of the line pair patterns revealed considerable differences between scanning protocols. Whereas subjective noise was identical between protocols, Protocol 4 showed superior sharpness in the axial plane, whereas Protocol 3 showed the highest sharpness in the trans-axial plane. Some consistency between voxel size and sharpness could be seen, as Protocol 1 (with a voxel size of 0.4 mm) showed the lowest overall score (5.5) and Protocols 3-4 (voxel size 0.2 mm) had the highest overall score (11.5) (Fig. 4).

High uniformity was found for Protocols 1-3, with differences in grey values being below 4% of the grey value range between air and PMMA. For protocol 4, this difference was 10.7% due to the smaller diameter of the FOV, which caused grey value shading due to the asymmetrical position of the phantom (see Discussion section).

Table 2 Image quality results for the SEDENTEXCT IQ phantom. Scanning protocols are denoted as P1-P4; details for each protocol are found in Table 1.

			Scanning protocol			
	Parameter		**P1**	**P2**	**P3**	**P4**
Contrast-detail	**Rods visible**	Aluminium	5	5	5	5
		Air	5	5	5	5
		HA 50	0	0	0	0
		HA 100	3	4	4	4
		HA 200	4	5	5	5
		PTFE	4	5	5	5
		POM	4	4	4	4
		LDPE	5	5	5	5
	Total score		30	33	33	33
CNR	**Contrast-noise ratio**	Aluminium	14.1	15.4	20.3	17.1
		Air	9.4	10.5	15.4	11.0
		HA 50	0.2	0.2	0.4	0.1
		HA 100	0.9	1.0	1.5	1.2
		HA 200	2.2	2.8	3.8	3.2
		PTFE	4.0	4.6	6.7	7.2
		LDPE	3.6	3.8	5.4	5.9
Line Pairs	**Axial plane**					
	Individual lines	Group 1	0.5	1	1	1
		Group 2	0	0.5	0.5	1
	Distinguishable groups	0-10	0.5	1.5	1.5	2
	Overall sharpness	0-2	0	1	1	1.5
	Overall noise	0-2	1	1	1	1
	Total score axial		2	5	5	6.5
	Trans-axial plane					
	Individual lines	Group 1	1	1	1	1
		Group 2	0	0	1	0.5
	Distinguishable groups	0-10	1	1	2	1.5
	Overall sharpness	0-2	0.5	0.5	1.5	1
	Overall noise	0-2	1	1	1	1
	Total score trans-axial		3.5	3.5	6.5	5
Uniformity	**Largest difference**	Grey values	34	20	26	115
		%	3.77	2.29	2.69	10.7
		SDNR	0.33	0.23	0.30	1.62
	Central vs. peripheral	Grey values	32	14	6	62
		%	3.53	1.59	0.58	5.75
		SDNR	0.33	0.23	0.31	1.79
Metal artefacts	**Normalized SD (%)**	Titanium	3.8	3.2	3.8	7.5
		Lead	6.9	5.9	5.9	5.9

Metal artefacts, in terms of SD_{norm}, were similar for lead (5.9-6.9). For titanium, more severe artefacts were found for Protocol 4 (7.5) than for the other three protocols (3.2-3.8). The non-normalized SD was, on average, 77% higher for lead than for titanium.

Table 3 shows geometric accuracy results obtained using the QRM phantom. Two anterior-posterior and two left-right directions at each protocol were measured for three times yielding the total of twelve measurements. Protocol 1 (0.4 mm voxel size) and Protocol 2 (0.25 mm voxel size) yielded overall average errors of 0.08 mm and 0.04 mm, respectively. Likewise, Protocols 3 and 4, with a 0.2 mm voxel size, yielded an overall average error of 0.06 mm. The lowest and highest average errors were 0.03 mm and 0.14 mm, respectively, while the lowest and highest maximum errors were 0.04 mm and 0.25 mm.

Radiation dose

The dose-area product for Protocol 1-4 was 897.1 $mGy.cm^2$, 1058.4 $mGy.cm^2$, 474.1 $mGy.cm^2$ and 424.4 $mGy.cm^2$, respectively

Discussion

In this study a novel CBCT model, developed and distributed in Thailand was evaluated. The main purpose of the evaluation was to assess the performance of the CBCT unit in terms of image quality and radiation dose, ensuring that it is suitable for clinical use. While the evaluation of diagnostic image quality is outside of the scope of this study, a technical evaluation of image quality, as well as an evaluation of patient dose, is an essential aspect of quality assurance of radiological equipment, both during acceptance,

Table 3 Geometric accuracy results for the QRM-ConeBeam phantom. Scanning protocols are denoted as P1-P4; details for each protocol are found in Table 1. Abs = absolute, Max = maximum.

Protocol	Direction	Actual Length (mm)	Measured Length (mm)			Abs Error (mm)	Max Error (mm)	% Abs Error
			#1	#2	#3			
P1	A-P	140	140.03	139.98	140.03	0.03	0.03	0.02%
	A-P	120	119.96	120.01	119.96	0.03	0.04	0.03%
	L-R	140	139.93	139.86	139.81	0.13	0.19	0.10%
	L-R	120	119.9	119.93	119.75	0.14	0.25	0.12%
P2	A-P	140	139.97	140.04	139.94	0.04	0.06	0.03%
	A-P	120	120.02	119.95	120.04	0.04	0.05	0.03%
	L-R	140	139.99	139.98	139.91	0.04	0.09	0.03%
	L-R	120	119.95	119.96	119.93	0.05	0.07	0.04%
P3	A-P	100	100.08	100.07	100.09	0.08	0.09	0.08%
	A-P	80	80.04	79.96	79.98	0.03	0.04	0.04%
	L-R	100	99.97	100.09	99.98	0.05	0.09	0.05%
	L-R	80	79.96	79.9	79.91	0.08	0.10	0.10%
P4	A-P	60	60.1	59.98	59.95	0.06	0.10	0.09%
	A-P	40	40.02	39.93	39.99	0.03	0.07	0.08%
	L-R	60	59.94	59.98	59.92	0.05	0.08	0.09%
	L-R	40	39.93	39.92	39.95	0.07	0.08	0.17%

commissioning and routine testing throughout the lifetime of the equipment.

Interpretation of the image quality findings is somewhat complicated due to the fact that it is not possible to determine universal ranges, investigation levels or suspension levels for technical image quality parameters. Previous research has shown considerable variability in image quality between CBCT models (Pauwels et al., 2012a), despite the fact that all of these units are in clinical use. It can be foreseen that future studies will address this issue. At this moment, the image quality measurements mainly serve as a means to identify severe issues in terms of sharpness, noise, contrast and artefacts.

When comparing the overall performance of the 4 scanning protocols, it can be seen that Protocols 3 (for a full single jaw scan) and 4 (for a localized or dentoalveolar scan) are preferred owing to their much lower radiation dose, increased sharpness and higher contrast-to-noise ratio. While the lower dose can be explained by the smaller FOV, and the increased sharpness by the smaller voxel size, it is somewhat surprising that CNR values were higher for Protocols 3 and 4, as one would expect larger voxel sizes to correspond with lower noise. A possible explanation for the higher CNR for Protocols 3 and 4 is the reduced amount of X-ray scatter, which is directly proportional with the FOV size. In terms of contrast-detail, however, no differences were found between Protocols 2-4, whereas Protocol 1 showed a worse visibility of medium-contrast materials. None of the scans were able to resolve the HA 50 pattern due to its very low contrast with PMMA, which is in agreement with previous findings (Pauwels et al., 2012a). As a general interpretation of the overall performance of each protocol, it can be suggested that Protocols 1 and 2 should only be used if the region of interest dictates the use of a large FOV (e.g. orthognatic surgery).

Comparing the DAP results with the UK HPA survey (HPA, 2010a), it can be seen that doses from the DentiiScan 2.0 are roughly found between the 40^{th} and 90^{th} percentile of the 'raw' DAP data of the CBCT units found in the UK. However, when normalizing the doses to a 4 × 4 cm beam area (as was done in the

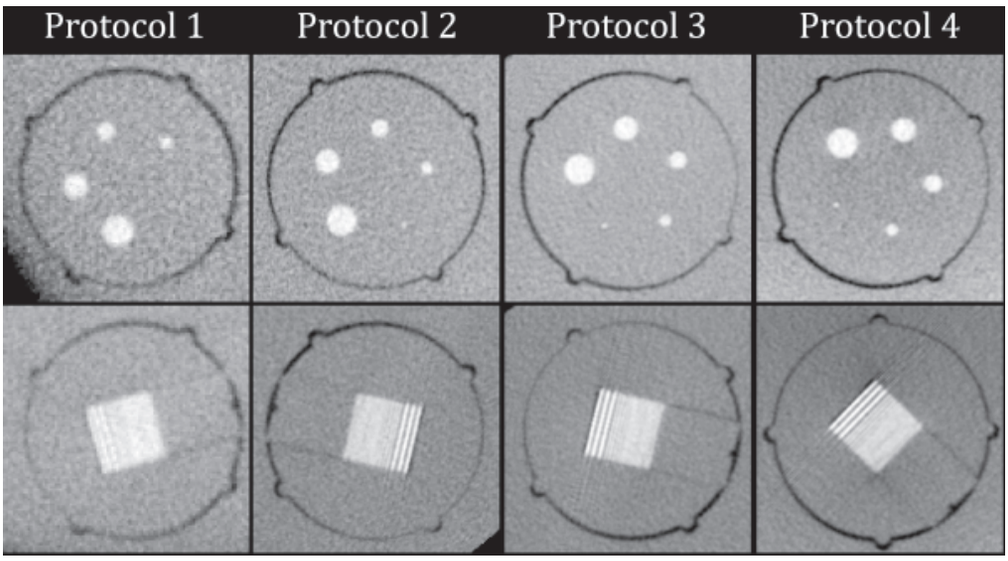

Figure 4 Selected slices illustrating the contrast-detail (top) and line pair (bottom) patterns of the SEDENTEXCT phantoms used in this study. Only one material (i.e. PTFE) used for the contrast analysis, and one orientation (i.e. axial) used for the spatial resolution evaluation is shown. All scans are displayed using an automatic window-level setting. Images were not rotated to avoid image quality degradation due to interpolation.

HPA study in order to determine the 'achievable dose'), values are between 69.0 and 107.5 mGy.cm^2, which is far below the proposed achievable dose of 250 mGy.cm^2, indicating that the tube output of the DentiiScan 2.0 is at the low-dose end of the CBCT spectrum. Future iterations of the machine should focus on the implementation of size-specific exposure settings (e.g. for children), as well as the possibility of adding a smaller FOV (e.g. 6 × 6 cm) for clinical applications such as single implants and endodontic treatment planning.

High grey value uniformity was seen for all protocols except Protocol 4. It has been shown before (both theoretically and experimentally) that smaller FOVs have increased uniformity issues due to the 'local tomography' or 'exo-mass' effect, which takes place if part of the scanned object is found outside of the FOV (Bryant et al., 2008). However, poor grey value uniformity does not necessarily affect diagnostic image quality, unless grey values are used in a quantitative way to estimate density such as in CT, where Hounsfield Units (or CT numbers) can be calibrated to bone mineral density (BMD). It should be taken into account that high uniformity does not imply that grey values can be used as Hounsfield Units (HU), as this is dependent on the presence or absence of HU calibration, the amount of scatter and beam hardening, and other factors. Clinical users are therefore not advised to use grey values in a quantitative way, unless the CBCT manufacturer can assure that HUs are accurate and stable (Pauwels et al., 2015).

Geometric accuracy for all protocols was in the range of 0.03-0.14 mm for the average absolute error and 0.03-0.25 mm for the average maximum error. These results confirmed that the average and maximum error of each protocol did not exceed two voxel sizes. Whereas prior guidelines have proposed that CBCT images should be accurate at a level of 0.5 mm (HPA 2010b, EC 2012), experimental studies and more recent guidelines have indicates that this may be too stringent, and that accuracy within 1.0 mm could be considered acceptable (de Las Heras Gala 2017). Although CBCT images are inherently more accurate than intra-oral, panoramic or cephalometric radiographs owing to the added dimension (i.e. 3D vs. 2D), users should take some degree of uncertainty into account when performing geometric measurements (e.g. bone width, distance to mandibular canal, root canal length).

Metal artefacts showed consistency between protocols, with one exception as mentioned above. The reason for this is that for Protocol 4, the insert containing titanium rods was scanned separately from the one containing lead rods. The normalization formula shown above takes the highest grey value in the FOV into account; for Protocol 4 this was equal to the grey value for titanium and lead for the scan of the titanium and lead inserts, respectively, whereas for the other protocols the highest grey values always corresponded to lead, irrespective of the insert under consideration. The higher SD value for Protocol 4 is therefore a result of a smaller effective grey value range for the titanium insert, and does not represent a true difference in imaging performance.

The results obtained in this study can be both used as reference values (during acceptance testing) and baseline values used throughout the lifetime of this particular model and unit. Identical measurements should be performed at regular intervals to ensure that image quality does not deteriorate excessively over time, and that radiation dose remains stable as well. Separate baseline values should be obtained for each installed unit before clinical use, and new baseline values should be measured whenever an extensive update or maintenance is performed.

In conclusion, the DentiiScan 2.0 showed adequate performance in terms of technical image quality. The radiation dose, normalized to the FOV size, was relatively low compared with other CBCT models. The protocol with the smallest FOV provided the best balance between image quality and dose.

Acknowledgements

RP is a paid consultant of the National Science and Technology Development Agency (NSTDA) of Thailand. ST, SA, CT, WN, PT are employees of the National Science and Technology Development Agency (NSTDA) of Thailand.

References

Bryant JA, Drage NA, Richmond S. Study of the scan uniformity from an i-CAT cone beam computed tomography dental imaging system. Dentomaxillofac Radiol. 2008;37:365-74.

de Las Heras Gala H, Torresin A, Dasu A, Rampado O, Delis H, Hernández Girón I, et al., Quality control in cone-beam computed tomography (CBCT) EFOMP-ESTRO-IAEA protocol (summary report). Phys Med. 2017;39:67-72.

EC, European Commission. Radiation Protection No 172: Cone beam CT for dental and maxillofacial radiology. Evidence based guidelines. Luxembourg: Office for Official Publications of the European Communities. 2012. https://ec.europa.eu/energy/sites/ener/files/documents/172.pdf

HPA, Health Protection Agency. Recommendations for the design of X-ray facilities and quality assurance of dental Cone Beam CT (Computed tomography) systems. HPA-RPD-065. Chilton, UK: Health Protection Agency. 2010a. https://www.gov.uk/government/uploads/system/uploads/attachment_data/file/348022/HPA-RPD-065_for_website.pdf

HPA, Health Protection Agency. Guidance on the safe use of dental cone beam CT equipment. HPA-CRCE-010 : Chilton, UK: Health Protection Agency. 2010b. https://www.gov.uk/government/uploads/system/uploads/attachment_data/file/340159/HPA-CRCE-010_for_website.pdf

Kamburoğlu K. Use of dentomaxillofacial cone beam computed tomography in dentistry. World J Radiol. 2015;7:128-30.

Kiljunen T, Kaasalainen T, Suomalainen A, Kortesniemi M. Dental cone beam CT: A review. Phys Med. 2015;31:844-60.

Nemtoi A, Czink C, Haba D, Gahleitner A. Cone beam CT: a current overview of devices. Dentomaxillofac Radiol. 2013;42:20120443.

Pauwels R, Stamatakis H, Manousaridis G, Walker A, Michielsen K, Bosmans H, et al., Development and applicability of a quality control phantom for dental cone-beam CT. J Appl Clin Med Phys. 2011;12:3478.

Pauwels R, Beinsberger J, Stamatakis H, Tsiklakis K, Walker A, Bosmans H, et al., Comparison of spatial and contrast resolution for cone-beam computed tomography scanners. Oral Surg Oral Med Oral Pathol Oral Radiol. 2012a;114:127-35.

Pauwels R, Beinsberger J, Collaert B, Theodorakou C, Rogers J, Walker A, et al., Effective dose range for dental cone beam computed tomography scanners. Eur J Radiol. 2012b;81:267-71.

Pauwels R, Stamatakis H, Bosmans H, Bogaerts R, Jacobs R, Horner K, et al., Quantification of metal artifacts on cone beam computed tomography images. Clin Oral Implants Res. 2013;24 Suppl A100:94-9.

Pauwels R, Silkosessak O, Jacobs R, Bogaerts R, Bosmans H, Panmekiate S. A pragmatic approach to determine the optimal kVp in cone beam CT: balancing contrast-to-noise ratio and radiation dose. Dentomaxillofac Radiol. 2014;43:20140059.

Pauwels R, Jacobs R, Singer SR, Mupparapu M. CBCT-based bone quality assessment: are Hounsfield units applicable? Dentomaxillofac Radiol. 2015;44:20140238.

Thongvigitmanee SS, Pongnapang N, Aootaphao S, Yampri P, Srivongsa T, Sirisalee P, et al., Radiation dose and accuracy analysis of newly developed cone-beam CT for dental and maxillofacial imaging. Conf Proc IEEE Eng Med Biol Soc. 2013;2013:2356-9.

Widmann G, Bischel A, Stratis A, Bosmans H, Jacobs R, Gassner EM, et al., Spatial and contrast resolution of ultralow dose dentomaxillofacial CT imaging using iterative reconstruction technology. Dentomaxillofac Radiol. 2017: 20160452.